Available online at www.sciencedirect.com
SCIENCE DIRECT®
Applied Energy 83 (2006) 687–704
APPLIED ENERGY
www.elsevier.com/locate/apenergy

Development of a thermoelectric battery-charger with microcontroller-based maximum power point tracking technique

Jensak Eakburanawat [a,*], Itsda Boonyaroonate [b]

[a] *Division of Energy Technology, School of Energy and Materials, Faculty of Engineering, King Mongkut's University of Technology Thonburi, Bangmod, Tungkru, Bangkok, Thailand*
[b] *Department of Electrical Engineering, Faculty of Engineering, King Mongkut's University of Technology Thonburi, Bangmod, Tungkru, Bangkok, Thailand*

Received 8 April 2005; received in revised form 27 May 2005; accepted 4 June 2005
Available online 11 October 2005

Abstract

This article describes a battery charger, which is powered by thermoelectric (TE) power modules. This system uses TE devices that directly convert heat energy to electricity to charge a battery. The characteristics of the TE module were tested at different temperatures. A SEPIC dc–dc converter was applied and controlled by a microcontroller with the maximum power point tracking (MPPT) feature. The proposed system has a maximum charging power of 7.99 W: that is better than direct charging by approximately 15%. The objectives are to study the principle of TE power generation and to design and develop a TE battery charger that uses waste heat or another heat source as the direct input power.

Keywords: Thermoelectric generator; dc–dc converter; SEPIC; MPPT

* Corresponding author. Tel.: +662 470 9051; fax: +662 470 9033.
E-mail address: Jensak@engineer.com (J. Eakburanawat).

0306-2619/$ - see front matter © 2005 Elsevier Ltd. All rights reserved.
doi:10.1016/j.apenergy.2005.06.004

Nomenclature

A	cross-sectional area of thermoelement $(mm)^2$
D	% duty cycle of gate signal
I_L	load current (A)
L	length of the thermoelement (mm)
L_C	thickness of the contact layer (mm)
M	conversion ratio
N	number of thermoelements per module
n	electrical-contact parameter
P_o	power output (W)
r	thermal-contact parameter
R_{int}	internal resistance of TE generator (Ω)
R_L	load resistance (Ω)
r_i	input resistance at the maximum power point (Ω)
T_c	cold-side temperature of module (°C)
T_h	hot-side temperature of module (°C)
V_i	input voltage of converter (V)
V_o	output voltage of converter (V)
v_i	input voltage at the maximum power point (V)
V_{oc}	open-circuit voltage of TE generator (V)

Greek symbols

α	thermoelectric material Seebeck coefficient (V/K)
ΔT	temperature difference (°C)
λ	thermal conductivity of thermoelement
λ_c	thermal conductivity of contact layer
ρ	electrical resistivity
ρ_c	contact resistivity between thermoelements and copper contacts
σ	material electric conductivity ($\Omega^{-1}\,cm^{-1}$)

Abbreviation

CCM	continuous-current mode
MPPT	maximum power point tracking
SEPIC	single-ended primary inductance converter
PWM	pulse width modulation

1. Introduction

Currently in Thailand, the electrical-power demand is increasing which prompts the government to build new power plants. Electrical energy is important for modern day living. However, some areas in Thailand do not have electricity and the residents desire some of the advantages and conveniences that electricity provides. Nowadays, the electrical power in remote areas is generated primarily by gasoline motor-generators. But, most people believe these generators are too noisy, require too much maintenance, and have high fuel costs [6].

Renewable energy, such as solar energy, wind energy or hydropower is preferred, but it has limited use and is dependent on weather and topography. Thermoelectrics can convert heat energy to electrical power directly. Thermoelectric power generation has the advantages of being maintenance free, silent in operation and involving no moving or complex parts.

In the past years, much work has been reported on the TE power generator. Killander [1] developed a stove-top generator using two TE power modules, model HZ-20. During the operating time, the output of the generator was about 10 W and supplied the battery with a net input from 1 to 5 W. Rahman [2] developed the thermoelectric generator to supply portable electronic equipment or to charge a lap-top computer battery. The generator is powered from butane gas; it has a potential power output of about 13.5 W. Roth et al. [3] developed and tested a photovoltaic/thermoelectric hybrid system as a power supply for a mobile telephone repeater. The developed system supplies enough for 50 W permanent loads. All of the above research uses the converter to boost-up the output voltage to charge the battery but do not use the maximum power point tracking control in the system.

2. Thermoelectric power generator

2.1. Theory of thermoelectric power generator

The TE effect was first discovered in 1822 by Seebeck, who observed an electric flow when one junction of two dissimilar metals, jointed at two places, was heated while the other junction was kept at a lower temperature [4]. A typical multicouple thermoelectric power module is shown schematically in Fig. 1: n-type and p-type semiconductor thermoelements are connected in series by highly-conducting metal strips to form a thermocouple. Based upon an improved theoretical model which takes into account the thermal and electrical contact resistance, the output voltage V_O, current I_O and power P_O when the module is operated with a matched load, are given by [5]:

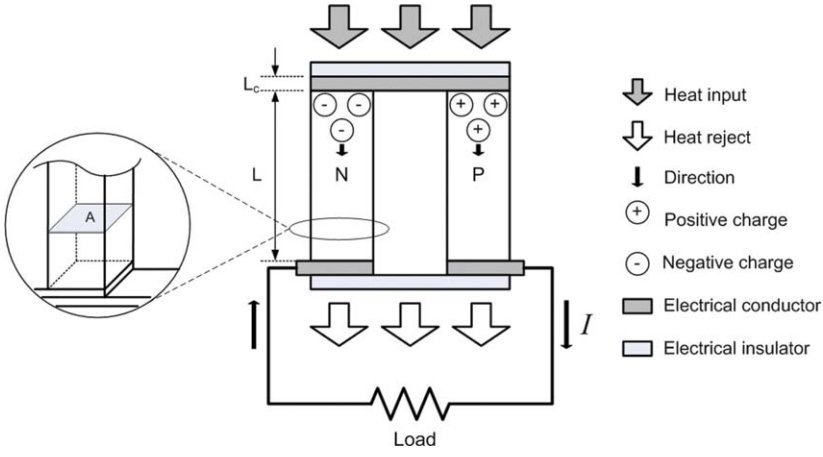

Fig. 1. Schematic of a single thermoelectric-couple.

$$V_O = \frac{\alpha N(T_h - T_c)}{1 + 2rL_C/L}, \tag{1}$$

$$I_O = \frac{\alpha A(T_h - T_c)}{2\rho(L+n)(1 + 2rL_C/L)}, \tag{2}$$

$$P_O = \frac{\alpha^2}{2\rho} \cdot \frac{NA}{(L+n)(1 + 2rL_C/L)^2} \cdot (T_h - T_c)^2, \tag{3}$$

where $n = 2\rho_C/\rho$, $r = \lambda/\lambda_C$, α is the TE material Seebeck coefficient (V/K), ρ is electrical resistivity (Ω cm), ρ_C is electrical contact resistivity, N is the number of the thermoelement in the module, A is the cross-sectional area of the thermoelements $(mm)^2$, L is the length of the thermoelement (mm), L_c is the thickness of the contact layer (mm), T_h is the temperature at the hot side, T_c is the temperature at the cold side, λ is the thermal conductivity of the thermoelement and λ_C is the thermal conductivity of the contact layer.

2.2. Thermoelectric module characteristics

TE power modules from Taihuaxing Co. Ltd. are used in the experiment. The specifications of the module are as follows.

- Part number TEP1-1264-1.5.
- Size: 40 mm × 40 mm.
- Open circuit voltage: 8.6 V.
- Internal resistance: 3 Ω.
- Match load output-voltage: 4.2 V.
- Match load output-current: 1.4 A.
- Match load output-power: 5.9 W.
- Heat flux across the module: about 140 W.
- Heat flux density: about 8.8 W/cm^2.

2.3. Finding the electrical characteristics of TEP1-1264-1.5

In this research, we designed and built the TE power generator (see Fig. 2). The electric heater is used as a heat source to supply heat energy to the hot side of TE modules. A heat sink was mounted on the cold side of the TE modules to maintain a constant temperature. The electrical characteristics of TEP1-1264-1.5 were tested by setting the hot-side temperature at 100, 125, 150, or 175 °C, and maintaining the cold-side temperature at 40 °C. A rheostat was connected to the thermoelectric modules as a load, and the resistance set at 1, 2, 3,..., or 10 Ω and the voltage and the current measured in each step. The voltage, current and power which 1 TE module can produce for each degree of temperature is shown in Figs. 3–5.

The variation of the output V–I characteristics of a TE module as a function of temperature differential (ΔT) between the hot side and cold side of the TE module is shown in Fig. 6. The ΔT changes affect mainly the TE output power.

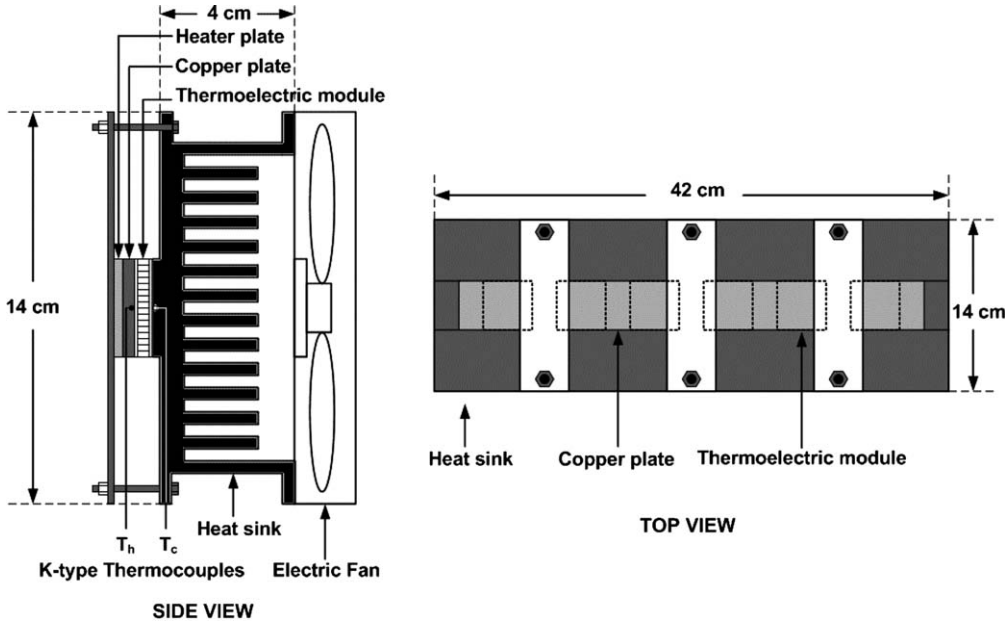

Fig. 2. The detail structure of a TE generator.

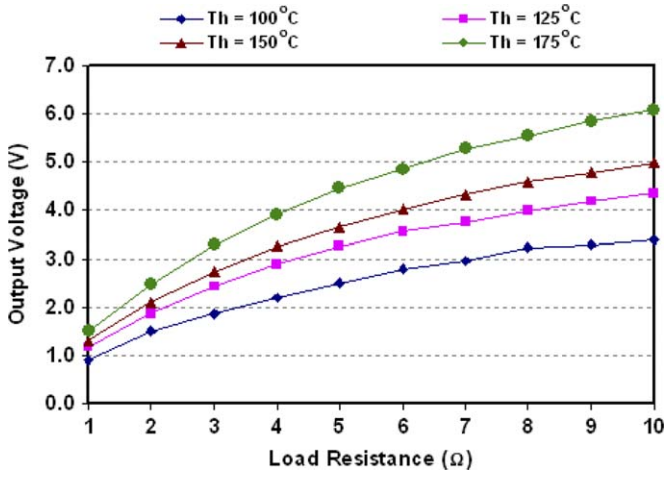

Fig. 3. Output voltage of single TE module (TEP1-1264-1.5) compared with load resistance at 40 °C cold-side temperature.

3. Converter and controller

3.1. Basic operation principle of the SEPIC converter

The SEPIC converter is a non-inverting dc–dc converter and can generate voltages either above or below the input. The input current is non-pulsating, but the output current

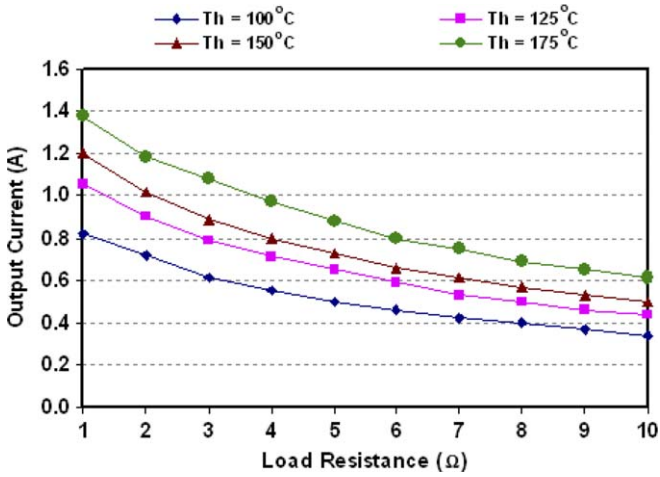

Fig. 4. Output current of single TE module (TEP1-1264-1.5) compared with load resistance at 40 °C cold-side temperature.

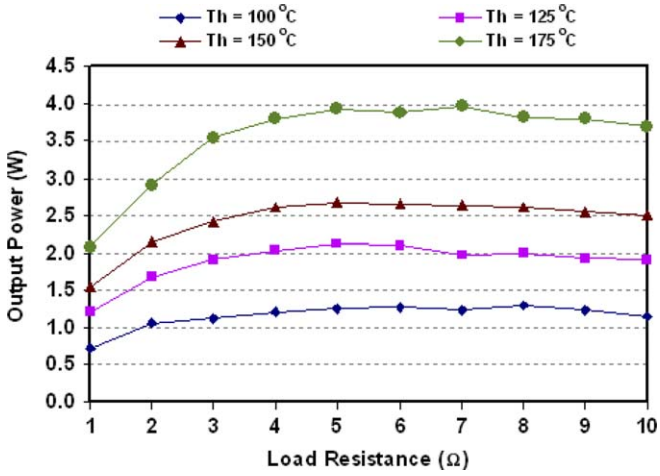

Fig. 5. Output power of single TE module (TEP1-1264-1.5) compared with load resistance at 40 °C cold-side temperature.

is pulsating. The name SEPIC is an acronym for single-ended primary inductance converter. A typical circuit diagram is shown in Fig. 7. This circuit has three dynamic energy storage elements, L_1, L_2 and C_1. The ratio of the output voltage to the input voltage and the duty cycle are defined as:

$$M = \frac{V_O}{V_i}, \tag{4}$$

$$D = \frac{t_{ON}}{T}. \tag{5}$$

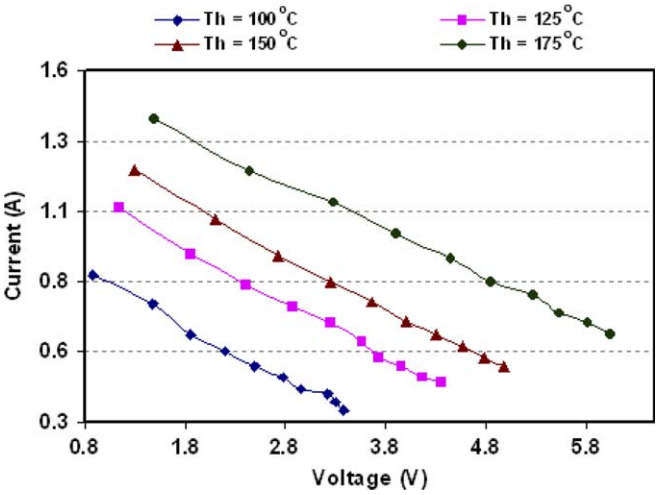

Fig. 6. *V–I* curve of a single TE module (TEP1-1264-1.5) at 40 °C cold-side temperature.

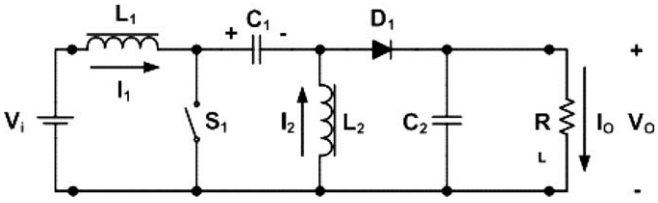

Fig. 7. A typical circuit diagram of the SEPIC DC–DC converter.

D as a function of M is:

$$D = \frac{M}{M+1} \tag{6}$$

and M as a function of D is:

$$M = \frac{D}{1-D} \tag{7}$$

By substituting (4) into (7), the output voltage can be expressed as:

$$V_O = \frac{D}{1-D} \cdot V_i, \tag{8}$$

where M is the conversion ratio of converter, V_i is the input voltage, V_o is the output voltage, and D is the percentage of the gate drive signal.

The behavior of any switchmode circuit is dependent on the continuity of the currents in the inductors and the voltage on the capacitor. In this research, the converter is operated in continuous-current mode (CCM); the sequence of operation and the waveforms being shown in Figs. 8 and 9.

3.2. System simulation

The proposed electrical behavior of the system operation was simulated using the Orcad PSpice Program [9]. The electrical model of the TE power generator in the circuit

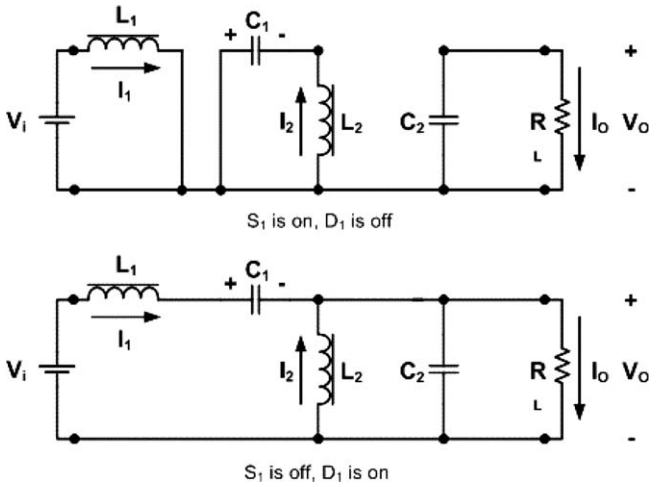

Fig. 8. Topology sequence of the SEPIC DC–DC converter.

simulation (see Fig. 10) was developed using the tested parameters of the TE power generator. It consists of a voltage source and a resistor connected in series. The value of a voltage source in the model is the open-circuit voltage of the TE power-generator and the

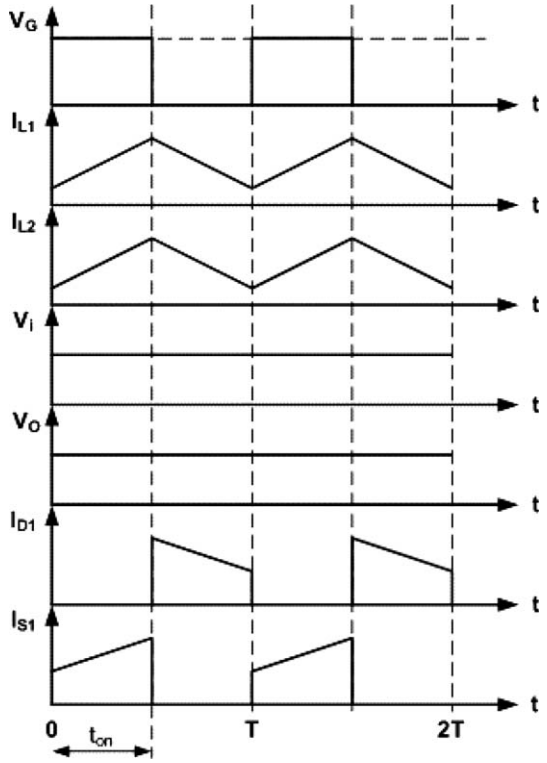

Fig. 9. Theoretical waveforms of the SEPIC DC–DC converter.

value of the resistor is the internal resistance of the TE power-generator. From Fig. 11, the procedure for testing is connecting 6 TE modules in series, input heat energy to the hot side of TE module, measuring the open-circuit voltage (V_{NL}), switching-on the S_1 to connect the R_L in the circuit and measuring the load current (I_L). Then, the internal resistance of the TE power-generator is calculated by:

$$V_{oc} = I_L \cdot (R_{int} + R_L), \tag{9}$$

$$R_{int} = \frac{V_{oc}}{I_L} - R_L, \tag{10}$$

where V_{oc} is the open-circuit voltage, I_L is the load current, R_L is the load resistance and R_{int} is the internal resistance (see Fig. 12).

From the test results of the TE power generator internal-resistance in Table 1, 17.8 Ω internal resistance and the 27.8 V open-circuit voltage were chosen for the electrical model of TE power generator. The simulation was at 18 kHz, 35% duty cycle of gate signal and the load was a 6 V battery with 0.1 Ω internal resistance (see Fig. 10). The simulation results for the input voltage, the input current, the output voltage and the output current of the dc–dc converter are shown in Fig. 13. The output power of the dc–dc converter that charges the battery was about 9 W.

3.3. Maximum power point tracking [6–9]

The TE battery-charger system was implemented by using the parameters from the simulated circuit. The maximum power point was changed as the temperature varies (see

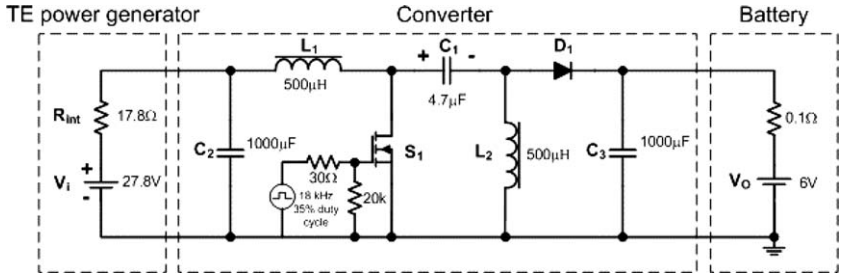

Fig. 10. The circuit diagram of the TE battery charger system for simulation.

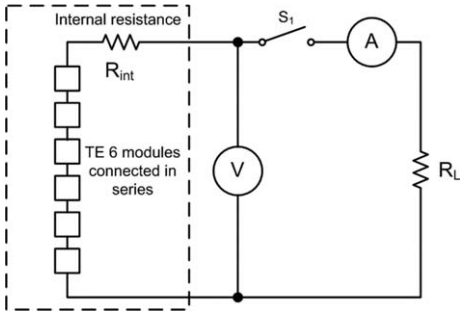

Fig. 11. The circuit diagram of the internal-resistance testing method.

Table 1
Testing results for the TE power generator internal-resistance

Module hot-side temperature (T_h), °C	Open-circuit voltage (V_{oc}), V	Load current (I_L), A	Internal resistance (R_{int}), Ω
90	13.00	0.55	13.63
100	14.20	0.60	13.67
110	16.50	0.70	13.57
120	18.00	0.75	14.00
130	19.80	0.80	14.75
140	21.20	0.85	14.94
150	23.20	0.90	15.78
160	24.90	0.95	16.21
170	26.00	0.98	16.53
180	27.80	1.00	17.80

$R_L = 10\ \Omega$; the module cold side temperature = 40 °C.

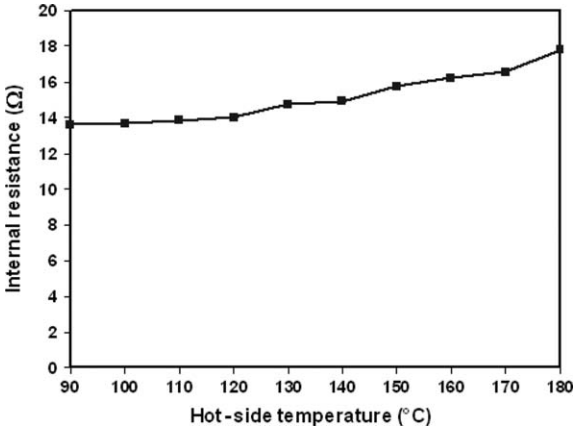

Fig. 12. The internal-resistance of the TE power generator.

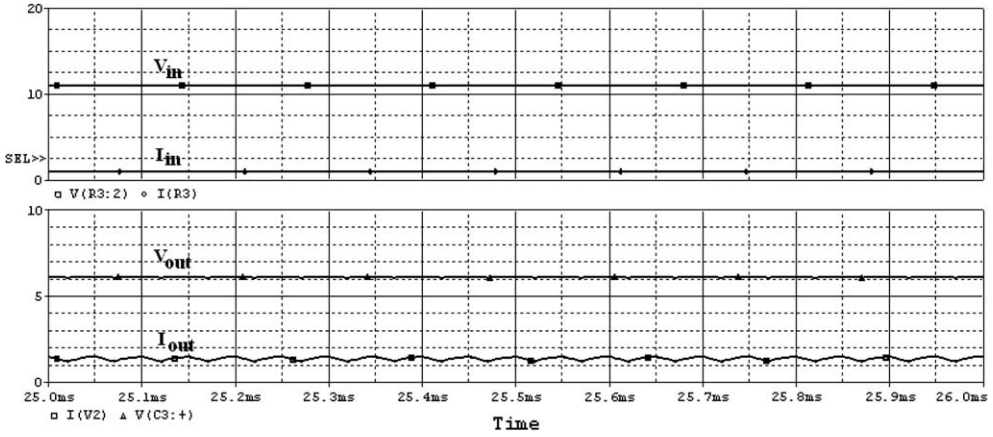

Fig. 13. The simulation results of the TE battery charger system.

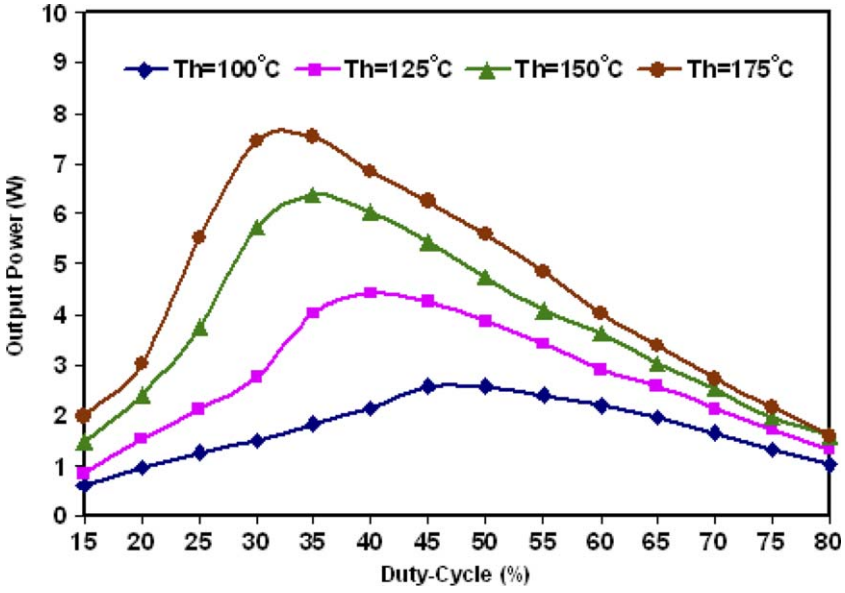

Fig. 14. The relation of duty cycle and output power which transfers to a battery.

Fig. 14). From Fig. 15, the maximum power transfer to the battery occurred when the input impedance of the dc–dc converter was equal to the output impedance of the TE power generator. The input impedance of the dc–dc converter can be controlled directly by changing the duty cycle of the gate driving signal; then we can find the maximum power point of the power transferred to the battery. The rate change of the input power with respect to input voltage and input resistance can be shown as follow [7]:

$$P_{\mathrm{i}} = P_{\mathrm{O}} = \frac{v_{\mathrm{i}}^2}{r_{\mathrm{i}}}, \tag{11}$$

$$\partial P_{\mathrm{i}} = \frac{2v_{\mathrm{i}}}{r_{\mathrm{i}}}\partial v_{\mathrm{i}} - \frac{v_{\mathrm{i}}^2}{r_{\mathrm{i}}^2}\partial r_{\mathrm{i}}. \tag{12}$$

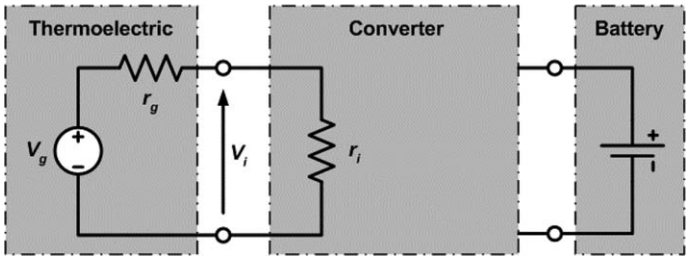

Fig. 15. Equivalent circuit of a thermoelectric power generator connected to a converter.

At the maximum power point, the rate change of the input power is zero. Hence

$$\partial P_{\mathrm{i}} = 0 \Rightarrow \frac{\partial v_{\mathrm{i}}}{\partial r_{\mathrm{i}}} = \frac{v_{\mathrm{i}}}{2r_{\mathrm{i}}}, \tag{13}$$

where v_{i} and r_{i} are input voltage and input resistance at the maximum power point respectively.

In the battery charging application, where the dc–dc converter output voltage can be assumed almost constant, a feed-forward MPPT controller may be applied [8]. The value of the battery-charging current is directly controlled by the duty cycle of the PWM control signal, which is applied to the dc–dc converter. An output power increase results in both a higher output current and a higher PWM control signal duty cycle, until the maximum power is transferred to the load.

4. Proposed system

A detailed circuit diagram of the proposed system is shown in Fig. 16. A SEPIC dc–dc converter is used to interface the TE power-generator output to the battery and to track the maximum power point of the TE power generator. The TE power generator consists of 6 TE power modules connected electrically in series and thermally in parallel, giving a 27.8 V open-circuit voltage at 180 °C hot-side temperature and 60 °C cold-side temperature. The SEPIC dc–dc converter consists of a RFP50N06 power MOSFET rated at 60V 50A $R_{\mathrm{ds(ON)}} = 0.022\ \Omega$, the fast-switching type diode D_1, the capacitor values are $C_1 = 4.7\ \mu\mathrm{F}$, C_2 and the inductors $C_3 = 1000\ \mu\mathrm{F}$, the inductors values are L_1, $L_2 = 500\ \mu\mathrm{H}$ and the inductors are wound on a ferrite core. The output of a SEPIC dc–dc converter is connected to A 6 V, 12 Ah battery.

The MPPT control-system consists of the 8-bit ATMEL microcontroller unit T89C51AC2 and features 5-I/O port, 8-bit PWM on-chip, 10-bit resolution A/D converter with 8 multiplexed inputs and the signal conditioner. The microcontroller unit used by the control program measures the signals required for the power flow control. This type of

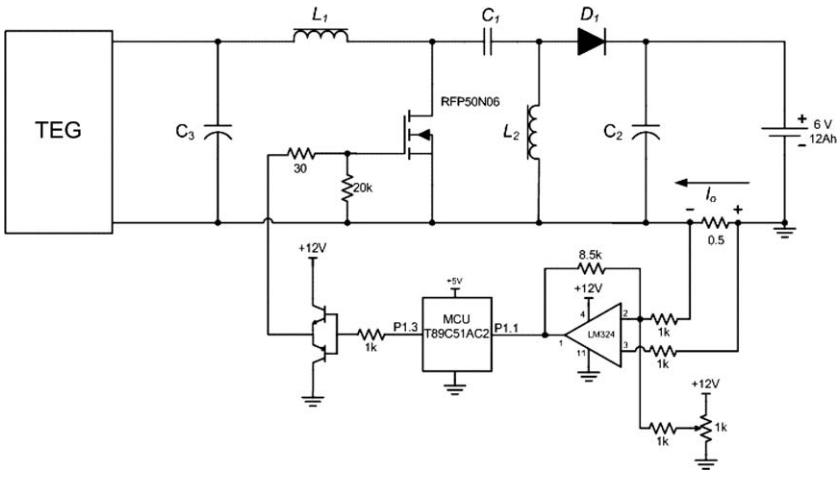

Fig. 16. The proposed system's circuit-diagram.

microcontroller was chosen because it has the necessary features for the proposed system, such as an on-chip A/D converter, PWM output, high clock rate, low power consumption and low cost.

The signal conditioner consists of a 0.5 Ω carbon-metal film resistor connected in series with the battery to measure the charged current from the system and send it to the non-inverting amplifier circuit. The output signal of a non-inverting amplifier is sent to the internal A/D converter of a microcontroller to convert it to digital data for use in the control program. The output PWM channel of a microcontroller is connected to the complementary transistors to amplify the output PWM signal. For higher accuracy, a Hall-effect sensor could be used. However, the Hall-effect sensor is more expensive.

The algorithm of the proposed program with the MPPT feature can be explained by the flowchart, which is shown in Fig. 17. The output of an A/D converter is used to calculate a PWM command duty cycle to drive a power switch. When the system starts operating, the program variable is set to an initial condition. The first PWM command is 25% duty cycle and the reference current I_{pass} is zero. The dc–dc converter starts operation and the current flows to the battery. The first signal captured from the signal conditioner is set to $I_{present}$ to compare it with the reference current I_{pass}. If $I_{present}$ is more than I_{pass}, the program increases the duty cycle. Then, the battery-charging current increases. The system operates at the maximum power point by adding the PWM command duty cycle. On the other hand, if I_{press} is more than $I_{present}$, then the duty cycle is over: the program goes to the next loop to decrease the duty cycle and returns to the previous loop when I_{pass} was more than $I_{present}$ again. Finally, the program can operate at the steady-state operation range automatically. The detailed MPP tracking process is shown in Fig. 18. The range of the 8-bit PWM is 256 steps that change the on time of the duty cycle. The Δd is a program variable with values either 1 or −1, indicating the direction that must be followed on the hill-shaped charging current curve.

5. Experimental and results

A prototype of a TE battery charger system has been developed and tested in the laboratory. The temperature was measured using K-type thermocouples which determine the hot-side and cold-side temperatures of the TE power modules. The K-type thermocouples were mounted just below the copper plate and the heat sink (see Fig. 2) and connected to a data logger which recorded one set of readings every 4 s. The power was recorded using a power analyzer (FLUKE 43B) to measure and record data every 4 s. The experimental procedures is as follows:

(a) Connect the TE power generator to a battery directly for direct charge. Switch-on the power supply to provide power to the heater. Start recording all data. The maximum power transfer to the battery is 6.35 W in the steady state.
(b) Connect the TE power generator to the input of the dc–dc converter and connect the output of the dc–dc converter to a battery; use a function generator to generate the 18 kHz 35% duty cycle drive gate signal provided to the power switch. Switch-on the power supply to provide power to the heater. Start recording all data. The maximum power transfer to the battery is 7.63 W in the steady state.

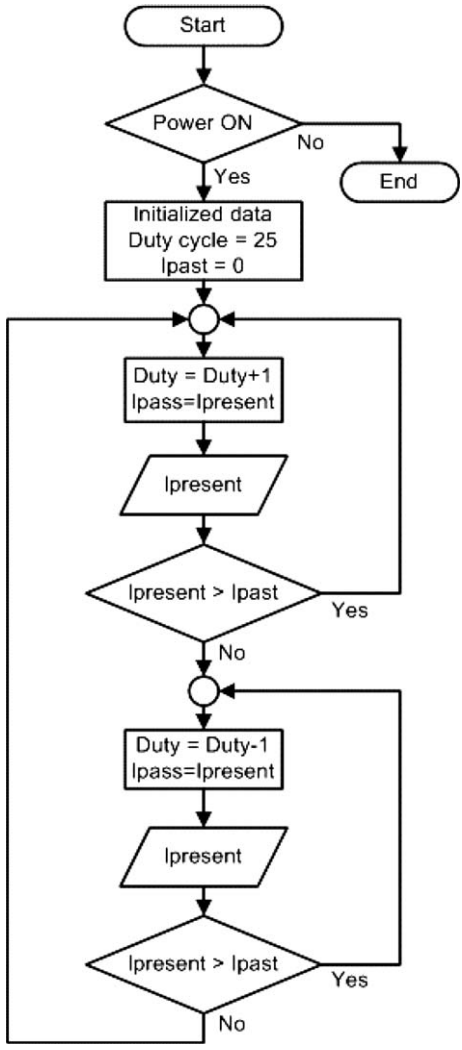

Fig. 17. Program flowchart of MPPT tracking process.

(c) Connect the MPPT control unit to the system to use the automatic control function. The maximum power transfer to the battery is up to 7.99 W in the steady state.

For the direct charging method, the system starts operation at the ambient temperature. The TE power generator could not produce a voltage because the temperature of the hot side and the cold side of TE were not different. Then, the TE module connected to the battery acted as the load. The current must flow to the TE power generator. Some loss of power was expected. For charging with the dc–dc converter, the converter topology has a flyback diode which can block the current flow up to the TE power generator. So, the

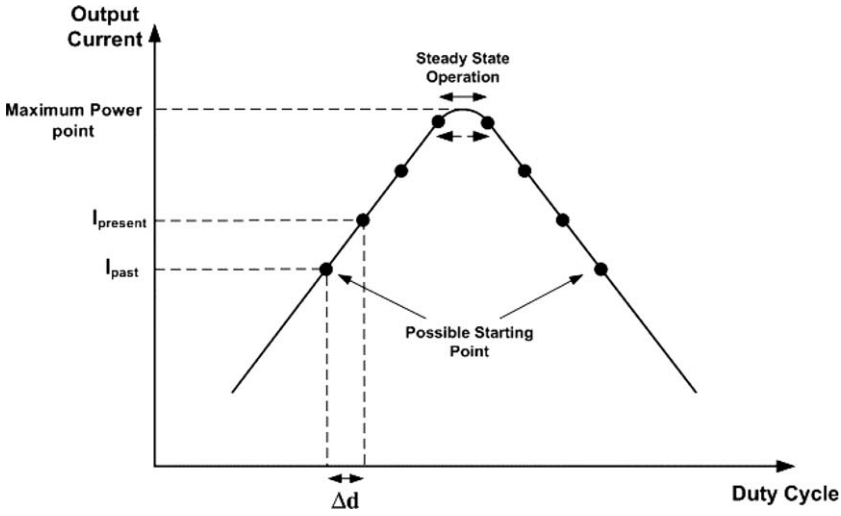

Fig. 18. The MPPT tracking process.

system can start operating although the generator voltage is less than the battery voltage. The hot-side and cold-side temperatures is shown in Fig. 19. A comparison of the battery charging power is shown in Fig. 20.

The maximum powers transfers from each method, i.e. direct charging, charging by using a dc–dc converter and charging using the dc–dc converter with MPPT control are 6.35, 7.63 and 7.99 W, respectively. The comparison of the power from each method is shown in Fig. 20. The input power measured at the front of the dc–dc converter is about 8.4 W. It is the maximum power that the dc–dc converter can get from the TE power

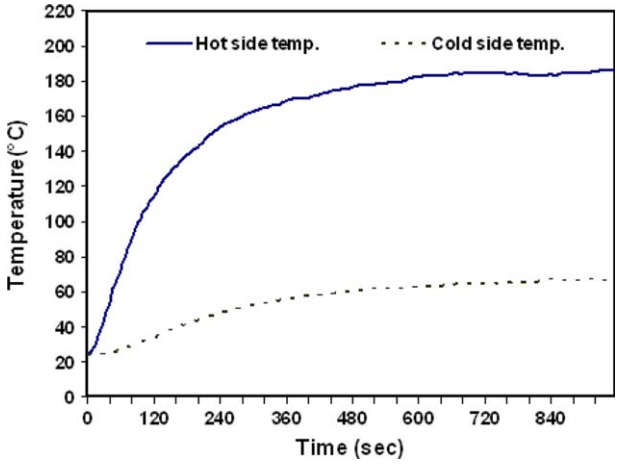

Fig. 19. The comparison of hot-side and cold-side temperatures of the TE power module.

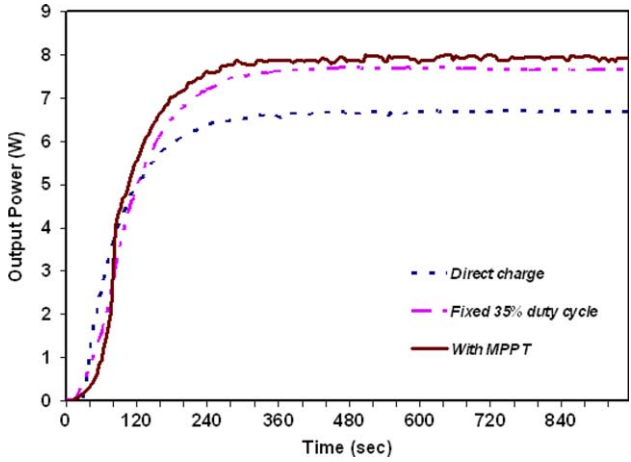

Fig. 20. The battery charging power.

generator, namely the power source and the load matches. The output power of the dc–dc converter is 7.99 W. The efficiency of the dc–dc converter is 95.11% when using the MPPT control. It is better than the direct charging method by about 15%.

Using the same experimental procedure, we staggered the heat supply at intervals; (switch-on the heater power supply 6 min, switch-off 2 min and switch-on again) providing the heat to the TE power generator. The comparisons of the battery charging power are shown in Fig. 21. The waveform of gate signal, input and output current of the dc–dc converter when using the MPPT control are shown in Fig. 22.

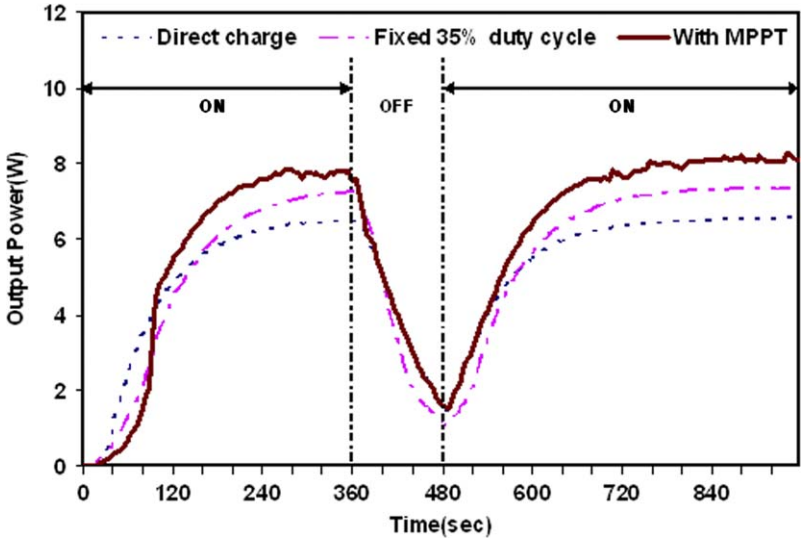

Fig. 21. Response of the battery charging power to turning the heat source off and on.

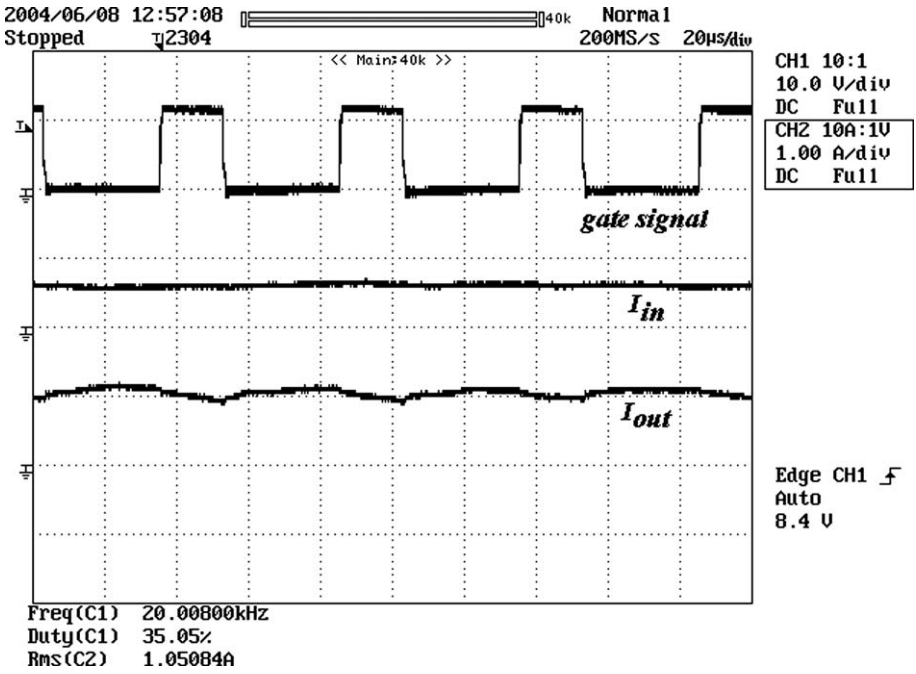

Fig. 22. The waveform of the gate signal; and the input and output currents of the dc–dc converter.

6. Conclusion

The advantage of the TE battery-charger system using MPPT is that the system can charge the battery by using the heat energy directly, and not having moving parts. It can be applied to heating devices such as a cook-stove, a boiler or another heat source for waste-heat recovery. This system is the most feasible to use in a rural community or a remote area. The photovoltaic system provides electrical power during sunshine, while the TE battery charger system provides power as long as the heating device is in use. The best power output of the system depends on the heat dissipation of the heat sink. However, the system design may be improved by redesigning the heat exchanger (heat receiver and heat sink) appropriate to the ambient temperature. The aim of this paper is to provide a new method for generating electrical power; it might not be economic initially, but the results derived here may lay a foundation for further investigations of TE battery charger systems.

References

[1] Anders Killander, John C Bass. A stove-top generator for cold areas. In: Proceedings of the IEEE 15th international conference on thermoelectrics; 1996. p. 390–3.
[2] Mahmudur R, Roger S. Thermoelectric power-generation for battery charging. In: Proceedings of the IEEE conference on energy management and power delivery, vol. 1; 1995. p. 186–91.
[3] Roth W, et al. Grid-independent power-supply for repeaters in mobile radio networks using photovoltaic/thermoelectric hybrid systems. In: Proceedings of the 16th international conference on thermoelectrics; 1997. p. 582–5.

[4] Min G, Rowe DM. Peltier devices as generators. CRC handbook of thermoelectrics. London: CRC Press; 1995 [Chapter 38].
[5] Rowe DM, Min G. Design theory of thermoelectric modules for electrical power generation. IEE Proc-Sci Meas Technol 1996;143(6):351–6.
[6] Eakburanawat J, Khedari J, Hirunlabh J, Daguenet M, Maneewan S, Teekasap S. Solar-biomass thermoelectric power generation simulation. In: Proceeding of 22nd international conference on thermoelectrics, La Grande Motte, Montpellier, France; 2003.
[7] Chung Henry Shu-Hung, Tse KK, Ron Hui SY, Mok CM, Ho MT. A novel maximum power point tracking-technique for solar panels using SEPIC or Cuk converter. IEEE Trans Power Electron 2003;18(3):717–24.
[8] Koutroulis Eftichios, Kalaitzakis Kostas, Voulgaris NC. Development of a microcontroller-based, photovoltaic maximum power point tracking control system. IEEE Trans Power Electron 2003;16(1):717–24. 46–54, 2001.
[9] Orcad PSpice Version 9.2, Copyright 1986–1999 by Cadence Design Systems.